Contribution from the Center for the Study of Fast Transient Processes,
Department of Chemistry, University of Southern California, Los Angeles, California 90089-0482

Microwave Spectrum, Structure, and Dipole Moment of (Methylamino)diborane, $B_2H_5NHCH_3$

S. S. Durso, E. V. O'Gorman, J. R. Chow, A. B. Burg, and R. A. Beaudet*

Received May 21, 1987

The microwave spectra of nine isotopic species of (methylamino)diborane, $B_2H_5NHCH_3$, were observed and assigned between 8.0 and 40.0 GHz. The complete structure, except for the methyl group, has been determined by using the Kraitchman substitution method, giving the following structural parameters: r(B–B) = 1.916 ± 0.001 Å, r(B–N) = 1.538 ± 0.004 Å, r(N–H_N) = 1.010 ± 0.002 Å, r(N–H_μ) = 2.177 ± 0.006 Å, r(B-H_μ) = 1.365 ± 0.004 Å, r(B–H_{cis}) = 1.214 ± 0.008 Å, r(B–H_{trans}) = 1.188 ± 0.004 Å, ∠H_μ–N–H_N = 122.6 ± 1.1°, ∠H_{cis}–B–H_{trans} = 121.1 ± 0.3°, ∠B_1–N–B_2 = 77.0 ± 0.3°, ∠B_1–H_μ–B_2 = 89.1 ± 0.2°. The B_1–H_μ–B_2–N central ring is planar to within the experimental uncertainty (±1.0°). From the moments of inertia and the center of mass conditions for the methyl group, r(N–C) = 1.51 ± 0.01 Å and ∠C–N–H_μ = 127.7 ± 1.2°. No internal rotation splittings were detected. The dipole moment was determined to be 2.72 ± 0.03 D, by using Stark-effect measurements.

Introduction

This laboratory is continuing the study of the microwave spectra and molecular geometries of small substituted boron hydrides and carboranes. To explore the effects of terminal group substitution on the bridge structures in diborane derivatives, recently the molecules methyldiborane[1] and 1,1-dimethyldiborane[2] have been investigated.

Structural work has been carried out on diborane derivatives with heteroatom substitution in the bridge position, such as aminodiborane,[3] $B_2H_5NH_2$, and (dimethylamino)diborane,[4] $B_2H_5N(CH_3)_2$. In the latter compound, the nitrogen atom was located too close to the center of mass of the molecule to accurately determine any parameter containing the nitrogen atom. The accurate location of the nitrogen atom was resolved in the study of aminodiborane. A question that arose was whether the B_1–H_μ–B_2–N geometry would remain planar if an asymmetric methyl substitution were made at the nitrogen atom. To resolve this question and to complete the series, the rotational spectrum of (methylamino)diborane, $B_2H_5NHCH_3$, has been investigated.

Four distinct isotopically substituted samples, listed in Table I, were synthesized, and the microwave spectra of nine isotopic species of (methylamino)diborane were studied. This permitted the determination of the complete structure of (methylamino)-diborane, except for the methyl group, by using the Kraitchman substitution method. The absence of a ^{13}C-enriched sample prevented an accurate substitution structure to be calculated for the methyl group. However, an approximate structure of the methyl group was calculated by using two independent methods, namely fitting to the derived moments of inertia and fitting to the center-of-mass condition in the normal species of (methylamino)diborane. The final structure and the principal axis orientations of normal (methylamino)diborane are shown in Figure 1. The bridge hydrogen is referred to as H_μ, while the terminal hydrogens are designated H_{cis} and H_{trans}, depending on their positions with respect to the methyl group. The hydrogen attached to the nitrogen atom is referred to as H_N. Stark-effect measurements on selected transitions were carried out to obtain the dipole moment components μ_a, μ_c, and μ_{total}. No splittings of lines due to the internal rotation of the methyl group were observed.

MNDO (modified neglect of diatomic overlap) calculations were performed on the three amino compounds $B_2H_5NH_2$, $B_2H_5NHCH_3$, and $B_2H_5N(CH_3)_2$ in order to evaluate the predictive power of MNDO to accurately estimate structures of boranes. Better initial predictions for the expected transition frequencies of a particular molecule facilitate line assignments. Secondly, accurate, calculated values of the dipole moment components would aid appreciably in determining the general nature of the expected spectrum, by predicting whether the spectrum is predominantly a strong *a*, *b*, or *c* type. Results show that these MNDO calculations predict structures and dipole moment components of boranes reasonably well for microwave spectroscopy.

Table I. Measured Isotopic Species of $B_2H_5NHCH_3$[a]

sample no.	sample	species	rel isotopic abund
1	normal	11–11–14	0.64
		11–10–14	0.32
2	^{15}N	11–11–15	0.64
		11–10–15	0.32
3	D_N	11–11–14–D_N	0.64
		11–10–14–D_N	0.32
4	D_i	11–11–14–D_{cis}	0.26
		11–11–14–D_{trans}	0.26
		11–11–14–D_μ	0.13

[a] The relative abundance in each sample is statistically estimated and is based on a pure sample. D_i represents single-deuterium substitution of bridge or terminal hydrogens ($B_2H_4DNHCH_3$).

Experimental Section

All isotopically substituted samples of $B_2H_5NHCH_3$ were prepared by utilizing the original[5] synthetic procedure. Normal $B_2H_5NHCH_3$ was prepared by using 0.513 mmol of CH_3NH_2, which was converted to $CH_3NH_2{\cdot}BH_3$ by the action of diborane in slight excess, and treated with 9 mmol of diborane, flowing across it at 95–99 °C, at pressures no higher than $^1/_2$ atm. The calculated yield of H_2 was 0.51 mmol, but the actual yield of $B_2H_5NHCH_3$ was only 0.308 mmol (60%), the loss being explained by the formation of a white solid and a nonvolatile oil, presumably composed of $(CH_3NHBH_2)_3$. The desired material, easily purified by high-vacuum fractional condensation by using traps at −60 and −78 °C, had a vapor pressure of 47 Torr at 0 °C.

The ^{15}N-labeled and D_N-labeled samples were prepared by conventional methods. Both of these samples were essentially pure, and no normal $B_2H_5NHCH_3$ was detected in either sample by microwave spectroscopy. Designations used for the isotopic species are of the form B_1–B_2–N, while a fourth term represents the location of the deuterium atom substitution in monodeuteriated species. D_i (i = cis, trans, μ) represents the sample with single-deuterium substitution in the bridge or terminal hydrogen position ($B_2H_4DNHCH_3$). The D_i-labeled sample was prepared by deuterium exchange in the reaction of $B_2H_5NHCH_3$ with B_2D_6. The molar ratio was adjusted to give predominantly monodeuteriated product. The final sample consisted of mostly normal $B_2H_5NHCH_3$ with $B_2H_4DNHCH_3$ as the second most abundant species. The actual microwave spectrum contained lines assigned to 11–11–14, 11–10–14, 11–11–14–D_{cis}, 11–11–14–D_{trans}, and 11–11–14–D_μ, with numerous unidentified lines probably due to 11–10–14–D_{cis}, 10–11–14–D_{cis}, 11–10–14–D_{trans}, 10–11–14–D_{trans}, and 11–10–14–D_μ. The three D_i species of interest, where both B_1 and B_2 are ^{11}B, are also called D_{cis}, D_{trans}, and D_μ.

All samples were stored in liquid nitrogen, when not in use, to prevent thermal decomposition. All spectra were acquired by using Stark cells cooled with dry ice to prevent sample decomposition and possible hy-

(1) Chiu, C. W.; Burg, A. B.; Beaudet, R. A. *Inorg. Chem.* **1982**, *21*, 1204.
(2) Chiu, C. W.; Burg, A. B.; Beaudet, R. A. *J. Chem. Phys.* **1983**, *78*, 3562.
(3) Lau, K. K.; Burg, A. B.; Beaudet, R. A. *Inorg. Chem.* **1974**, *13*, 2787.
(4) Cohen, E. A.; Beaudet, R. A. *Inorg. Chem.* **1973**, *12*, 1570.
(5) Burg, A. B.; Randolf, C. L. *J. Am. Chem. Soc.* **1949**, *71*, 3451.

0020-1669/88/1327-0063$01.50/0

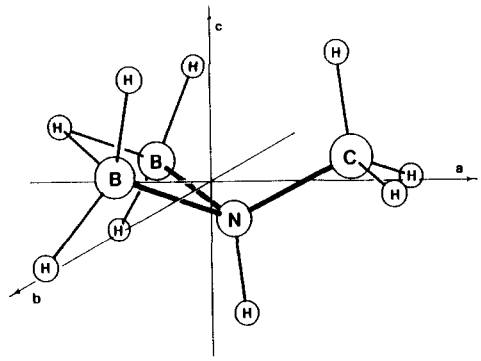

Figure 1. Molecular structure of (methylamino)diborane. Principal axis orientations are shown for the normal species.

drolysis with residual water adsorbed on the waveguide surfaces and the sample inlet tubing. Also, cooling to −78 °C simplies the microwave spectra by reducing absorption due to vibrationally excited species of $B_2H_5NHCH_3$. However, weak vibrational satellites, identified by Stark patterns identical with their analogous ground-vibrational-state lines, were observed. No evidence of internal rotation of the $-CH_3$ internal rotor was observed. No splitting of any of the lines, including those of unassigned vibrational satellites, was observed.

Once a Stark cell was conditioned with a particular isotopic sample, a fresh sample was not required to at least 4 h. For the case of the D_i sample, the labile hydridic deuterium exchanged readily with hydrogen on the walls of the waveguide to produce normal $B_2H_5NHCH_3$. This problem was considerably reduced by conditioning the waveguide with the D_i sample, thereby presumably saturating sites on the waveguide walls with deuterium. This technique required a fresh sample after an interval of about 2 h.

The rotational spectra in the 18.0–26.5-GHz region were recorded with a Hewlett-Packard 8460A MRR spectrometer and in the 26.5–40.0-GHz region with a Hewlett-Packard KII-8400B spectrometer, both Stark-modulated at 33 KHz. Gold-plated waveguides were used. Spectra in the 8.0–18.0-GHz region were observed with a home-built instrument with a 3-m copper Stark cell. Sample pressures varied between 0.02 and 0.08 Torr.

Spectra and Assignment

Rotational constants for (methylamino)diborane were initially estimated by using average values of bond lengths and bond angles obtained from $B_2H_5NH_2$ and $B_2H_5N(CH_3)_2$. These model calculations showed $B_2H_5NHCH_3$ to be an asymmetric prolate rotor, having a value of $\kappa = -0.60$ as its asymmetry parameter. Due to C_s symmetry, this molecule has both an a and a c dipole moment component unlike the other two amino analogues, which both have C_{2v} symmetry and thus only a single dipole component. Averaging the previously measured values for dipole moments of $B_2H_5NH_2$ and $B_2H_5N(CH_3)_2$ gives the approximate value of 2.70 D used for initial relative intensity calculations. Our model predicted mainly a strong a-type spectrum, with weaker c-type transitions. The initial search focused on the three $J = 2 \leftarrow 1$, a-type transitions, that is $2_{12} \leftarrow 1_{11}$, $2_{02} \leftarrow 1_{01}$, and $2_{11} \leftarrow 1_{10}$, which were predicted to be the most intense, low-J, R-branch transitions in the range of 18.0–26.5 GHz. A search in the expected frequency region resulted in relatively rapid assignments of these three transitions for the normal species. These lines, having clearly discernible Stark effects and appropriate relative intensities, were singled out of a moderately dense spectrum with the aid of the predicted asymmetry splitting pattern. Refined rotational constants were then used to calculate a more accurate spectrum, and the five $J = 3 \leftarrow 2$, a-type transitions, having higher relative intensities, were easily found in the 33–38-GHz range. These transitions were confirmed by their well-resolved Stark effects and served as comparison lines for selection and identification of analogous transitions in the recorded spectra for the other eight studies isotopic species.

Once the experimental rotational constants of the normal species were found, rotational constants for the 11–10–14 species were calculated by estimating the atomic coordinates. The $J = 2 \leftarrow 1$ and $J = 3 \leftarrow 2$ a-type transitions were readily found near their predicted positions, and these lines were lower in intensity than normal-species lines by approximately a factor of 2, as expected from simple statistical calculations. Similarly for the isotopically substituted species shown in Table I, estimated values guided spectral searches and strong a-type $J = 3 \leftarrow 2$ and $J = 2 \leftarrow 1$ transitions were observed for the remaining seven isotopic species. Attempts to observe both $J = 3 \leftarrow 2$ and $J = 2 \leftarrow 1$ transitions for the doubly ^{10}B substituted 10–10–14 species were not successful, presumably due to its small natural isotopic abundance of $^1/_{16}$ with respect to that of the normal species. Numerous high-J lines and Stark lobes also interfered with weak candidate lines in the region where the 10–10–14 species was expected to absorb. Many Q-branch and R-branch transitions of high-J lines up to $J = 31$, for most of the studied isotopic species, have been assigned, and their frequencies are available from the authors.

Of the weaker c-type transitions, the $2_{11} \leftarrow 1_{01}$ transition was observed with well-resolved Stark lobes at values of Stark fields up to 2000 V/cm for all except the D_i-substituted species (monodeuteriation in the bridge or terminal hydrogen position). This assignment facilitated calculation of better values of the A constants. Subsequently, additional c-type transitions were observed and identified by their Stark patterns. The $1_{01} \leftarrow 0_{00}$ a-type transitions were found within 1 MHz of their calculated positions for the six ^{14}N, ^{15}N, and D_N species. However, the weaker $1_{10} \leftarrow 0_{00}$ c-type lines, reduced by more than a factor of 2 in relative intensities, were not assigned. Table II lists assigned transition frequencies for ^{14}N and ^{15}N species, while Table III lists values for all monodeuteriated species. Only the $1_{01} \leftarrow 0_{00}$ transition was slightly broadened by nuclear quadrupole coupling of the boron and nitrogen nuclei to the molecular rotation. However, since the magnitude of these effects was small, no splittings were resolvable.

Values of the ground-vibrational-state rotational constants were calculated by using a least-squares fitting of assigned transitions to a rigid asymmetric rotor. Frequency deviations of 1–2 MHz resulted for the c-type $3_{31} \leftarrow 3_{21}$ and $3_{30} \leftarrow 3_{22}$ transitions when they were incorporated into the least-squares program along with all low-J lines up to $J = 3$. These deviations possibly reflect centrifugal distortion effects. For this reason these two transitions were excluded from the final data sets for the least-squares program, which consisted of all other low-J lines observed to $J = 3$. Since $B_2H_5NHCH_3$ has low-lying vibrational modes, owing mostly to the attached methyl group, centrifugal distortion effects are expected to contribute after $J = 5$ or 6. The frequency deviations reported in Tables II and III are interpreted as centrifugal distortion effects for these higher-J transitions. Since low-J transitions were used to obtain the rotational constants, centrifugal distortion effects were negligible. Deviations of several MHz for $J = 7$–12 and 10–20 MHz for $J = 31$ were noticed for lines assigned as Q- or R-branch, high-J transitions, with the observed frequencies usually lower in frequency than the calculated rigid-rotor values. Final least-squares-fitted values of the rotational constants, moments of inertia, and asymmetry parameters for all isotopic species observed are given in Table IV.

As mentioned above, the microwave spectrum of the D_i sample consisted of mostly nondeuteriated ^{14}N lines (11–11–14 and 11–10–14), as well as lines due to the three D_i species of interest, D_{cis}, D_{trans}, and D_μ. This spectrum proved to be more difficult to unravel than the spectrum of the other isotopic species since this sample contained at least 10 different isotopic species. Statistical considerations predicted relative intensity ratios of 2:2:1 for lines due to D_{cis}, D_{trans}, and D_μ, respectively. These ratios, along with calculated transition frequencies and Stark effects, assisted species assignments and were confirmed for the final reported values of both $J = 3 \leftarrow 2$ and $J = 2 \leftarrow 1$ transition frequencies for each of these three species. The predicted asymmetry splitting pattern of the $J = 3 \leftarrow 2$ transitions proved especially helpful in selecting candidate lines for closer scrutiny. The central lines $3_{03} \leftarrow 2_{02}$, $3_{22} \leftarrow 2_{21}$, and $3_{21} \leftarrow 2_{20}$ formed a triplet with nearly equal spacings, differing by only a few tenths of a megahertz. The actual spacings varied anywhere between 700 and 1000 MHz for a given species, depending on the value of the asymmetry parameter, as can be seen in Tables III and IV. Although the strong a-type J

Table II. Frequencies (MHz) of Assigned Rotational Transitions in ^{14}N and ^{15}N Isotopic Species of $B_2H_5NHCH_3$[a]

	11-11-14		11-10-14		11-11-15		11-10-15	
transition	ν_{obsd}	Δ	ν_{obsd}	Δ	ν_{obsd}	Δ	ν_{obsd}	Δ
				a Type				
$1_{01} \leftarrow 0_{00}$	11776.94	0.05	11947.60	0.18	11758.51	0.08	11929.53	0.13
$2_{12} \leftarrow 1_{11}$	22171.78	0.04	22536.52	0.19	22151.17	0.05	22516.79	0.18
$2_{02} \leftarrow 1_{01}$	23319.03	0.04	23675.01	0.15	23286.02	0.06	23642.66	0.13
$2_{11} \leftarrow 1_{10}$	24935.86	0.03	25253.41	0.08	24882.59	−0.01	25201.01	0.03
$3_{13} \leftarrow 2_{12}$	33121.54	0.05	33676.73	0.16	33092.82	0.03	33649.03	−0.08
$3_{03} \leftarrow 2_{02}$	34433.14	−0.01	34997.96	−0.09	34392.57	0.28	34958.02	0.10
$3_{22} \leftarrow 2_{21}$	35330.71	0.04	35842.15	−0.10	35275.48	0.19	35788.27	0.08
$3_{21} \leftarrow 2_{20}$	36228.11	−0.08	36686.41	−0.03	36157.89	−0.40	36618.22	−0.24
$3_{12} \leftarrow 2_{11}$	37242.53	0.27	37729.68	0.22	37165.76	0.59	37653.53	−0.02
$5_{24} \leftarrow 5_{05}$	30086.51	−0.40	30585.46	−0.55	29831.60	−0.61	30323.88	−0.81
				c Type				
$2_{11} \leftarrow 1_{01}$	31669.86	0.37	32170.43	0.47	31566.61	0.17	32065.82	0.23
$3_{21} \leftarrow 3_{13}$	23542.58	0.10	23979.66	−0.06	23347.86	−0.07		
$3_{31} \leftarrow 3_{21}$	29216.20	−0.81	30249.59	−1.04	29022.99	−1.89	30045.51	−1.34
$3_{30} \leftarrow 3_{22}$	30375.58	0.89	31338.22	0.81	30164.58	0.98	31118.05	2.56
$4_{04} \leftarrow 3_{12}$	*b*		34640.91	−0.13	33983.48	−0.07		
$4_{13} \leftarrow 3_{21}$	34043.30	−0.44	34141.37	−0.43	34043.59	−0.53		
$4_{32} \leftarrow 4_{22}$	27778.17	−0.09	28882.85	−0.04	27607.59	−0.25	28700.26	0.00
$4_{31} \leftarrow 4_{23}$	31110.65	−0.29	32022.87	−0.28	30887.10	−0.09	31789.21	−0.06
$5_{33} \leftarrow 5_{23}$	25432.79	−0.39	26624.80	−0.11	25294.43	−0.68	26474.29	−0.05
$5_{32} \leftarrow 5_{24}$	32707.64	−0.81	33507.77	−0.99	32456.03	−0.98	33247.72	−0.97
$6_{34} \leftarrow 6_{24}$	22278.69	−0.73	23548.87	−0.34	22180.23	−0.56	23438.29	−0.06

[a] Lines reported to 0.01 MHz have been measured to better than ±0.05 MHz; $\Delta = \nu_{obsd} - \nu_{calcd}$. [b] Interference by strong adjacent line.

Table III. Frequencies (MHz) of Assigned Rotational Transitions in Monodeuteriated Species of $B_2H_5NHCH_3$[a]

	11-11-14-D_N		11-10-14-D_N		11-11-14-D_{cis}		11-11-14-D_{trans}		11-11-14-D_μ	
transition	ν_{obsd}	Δ	ν_{obsd}	Δ	ν_{obsd}	Δ	ν_{obsd}	Δ	ν_{obsd}	Δ
					a Type					
$1_{01} \leftarrow 0_{00}$	11599.36	0.16	11767.67	0.34						
$2_{12} \leftarrow 1_{11}$	21988.38	−0.02	22351.33	0.04	21619.71	−0.13	21194.11	0.15	21421.36	−0.43
$2_{02} \leftarrow 1_{01}$	23003.46	0.05	23353.67	0.09	22745.96	0.17	22319.56	−0.05	22487.93	0.09
$2_{11} \leftarrow 1_{10}$	24408.67	0.26	24718.48	0.45	24427.45	−0.20	23946.21	0.07	23932.97	−0.08
$3_{13} \leftarrow 2_{12}$	32868.98	−0.19	33421.18	−0.08	32270.15	−0.19	31646.42	0.00	32022.15	0.19
$3_{03} \leftarrow 2_{02}$	34048.90	−0.09	34604.12	0.02	33489.48	0.50	32903.58	−0.12	33284.88	0.07
$3_{22} \leftarrow 2_{21}$	34797.36	−0.24	35301.90	−0.09	34535.07	−0.55	33855.15	0.08	34016.08	−0.05
$3_{21} \leftarrow 2_{20}$	35545.81	−0.41	35999.63	−0.25	35582.74	0.49	34806.32	−0.12	34747.57	0.12
$3_{12} \leftarrow 2_{11}$	36479.35	0.11	36954.17	0.36	36446.69	−0.14	35745.69	0.05	35770.66	−0.05
$5_{24} \leftarrow 5_{05}$	27335.09	−0.06								
					c Type					
$2_{11} \leftarrow 1_{01}$	30596.56	0.50	31063.93	−0.52	*b*		*b*		*b*	
$4_{04} \leftarrow 3_{12}$	34668.38	0.21								
$4_{31} \leftarrow 3_{21}$	34167.01	0.00								
$4_{32} \leftarrow 4_{22}$	25868.87	−0.10								
$4_{31} \leftarrow 4_{23}$	28654.19	0.02	29457.82	0.10						
$5_{33} \leftarrow 5_{23}$	23861.69	−0.42								
$5_{32} \leftarrow 5_{24}$	29969.58	−0.53	30669.91	−0.39						

[a] Lines reported to 0.01 MHz have been measured to better than ±0.05 MHz; $\Delta = \nu_{obsd} - \nu_{calcd}$. [b] Too weak to be observed.

Table IV. Rotational Constants, Moments of Inertia, and Asymmetry Parameters of the Isotopic Species of $B_2H_5NHCH_3$[a]

species	*A*, MHz	*B*, MHz	*C*, MHz	κ	mass, amu	I_a, amu Å^2	I_b, amu Å^2	I_c, amu Å^2
11-11-14	11931.09 (3)	6579.47 (2)	5197.42 (2)	−0.589 51	57.092 11	42.3582 (1)	76.8115 (2)	92.2365 (4)
11-10-14	12211.08 (3)	6652.96 (3)	5294.46 (2)	−0.607 18	56.095 74	41.3869 (1)	75.9630 (4)	95.4543 (4)
11-11-15	11880.19 (6)	6562.08 (4)	5196.35 (3)	−0.591 33	58.089 14	42.5396 (3)	77.0151 (4)	97.2565 (6)
11-10-15	12158.21 (3)	6635.79 (2)	5293.61 (2)	−0.608 95	57.092 78	41.5669 (1)	76.1596 (2)	95.4696 (3)
11-11-14-D_N	11382.25 (4)	6404.60 (2)	5194.60 (2)	−0.608 90	58.098 39	44.4006 (1)	78.9088 (3)	97.2893 (4)
11-10-14-D_N	11638.40 (7)	6475.35 (5)	5291.98 (5)	−0.627 07	57.102 02	43.4234 (2)	78.0466 (6)	95.4990 (9)
11-11-14-D_{cis}	11004.7 (21)	6457.89 (9)	5053.98 (9)	−0.528 15	58.098 39	45.9239 (88)	78.2576 (11)	99.9963 (17)
11-11-14-D_{trans}	11250.7 (7)	6330.56 (2)	4954.47 (2)	−0.562 89	58.098 39	44.9198 (28)	79.8316 (2)	102.0047 (4)
11-11-14-D_μ	11859.2 (17)	6297.17 (5)	5041.54 (5)	−0.631 65	58.098 39	42.6149 (61)	80.2549 (7)	100.2430 (10)

[a] Errors quoted are standard deviations from least-squares fits. A conversion factor of 505 379.05 amu Å^2 MHz was used. $\kappa = (2B - A - C)/(A - C)$.

$J = 3 \leftarrow 2$ and $J = 2 \leftarrow 1$ transitions and associated Stark effects were observed and confirmed for the D_{cis}, D_{trans}, and D_μ species, efforts to locate $2_{11} \leftarrow 1_{01}$ or any other *c*-type transition for these species failed. Again the spectra proved too weak for observation. Least-squares fits in these cases were comprised of eight *a*-type transitions. Although usually *c*-type transitions are required for improved determinations of the *A* rotational constant, the large asymmetry in the isotopic species of $B_2H_5NHCH_3$ results in *a*-type transitions that have higher dependence on the *A* rotational constant than a more symmetric molecule might otherwise have. A look at Table IV shows that asymmetry parameters vary from −0.5282 for D_{cis} to −0.5629 for D_{trans} and −0.6317 for D_μ species.

Table V. Stark Effect and Dipole Moment of Normal $B_2H_5NHCH_3$[a]

transition	M_J	$10^5(\Delta\nu/E^2)$	10^6A	10^6B
$2_{12} \leftarrow 1_{11}$	0	1.897 (4)	2.827	0.5444
	1	27.86 (7)	46.09	−6.203
$2_{02} \leftarrow 1_{01}$	0	−1.868 (9)	−3.289	1.396
	1	2.481 (12)	2.644	7.208
$2_{11} \leftarrow 1_{10}$	0	1.335 (2)	2.514	2.224
	1	−25.40 (16)	−42.51	1.132

$\mu_a = 2.50 \pm 0.02$ D, $\mu_c = 1.07 \pm 0.04$ D, $\mu_{total} = 2.72 \pm 0.03$ D

[a] $\Delta\nu/E^2$ units are MHz $(V/cm)^{-2}$, while A and B are in units of MHz $(V/cm)^{-2}$ D^{-2}. A and B are defined by the equation $\Delta\nu/E^2 = A\mu_a^2 + B\mu_c^2$.

The uncertainties in the A rotational constants would thus be expected to be smallest for D_{cis} and D_{trans} and somewhat larger for D_μ. The only molecule that behaves improperly in this sense is the D_{cis} species, which has a large standard deviation of ±2.1 MHz. As seen in Table III, D_{cis} also has comparatively larger frequency deviations from the rigid-rotor fit. The observed $3_{22} \leftarrow 2_{21}$ and $3_{21} \leftarrow 2_{20}$ transitions had very fast Stark effects, and thus they were appreciably broadened and were difficult to measure accurately. Since $3_{22} \leftarrow 2_{21}$ had the largest standard deviation in the least-squares fit, this line was omitted from a second fit, which contained only seven lines for the D_{cis} species. A much better fit resulted where deviations from observed transition frequencies were similar to values found for D_{trans} and D_μ. This calculation showed a considerably reduced uncertainty in the A constant of only ±0.60 MHz and lends support to the thought that difficulty in accurate line measurements may have contributed almost entirely to this inconsistency.

Dipole Moment

Stark-effect measurements were obtained on the three a-type $J = 2 \leftarrow 1$ transitions $2_{12} \leftarrow 1_{11}$, $2_{02} \leftarrow 1_{01}$, and $2_{11} \leftarrow 1_{10}$ of the normal $B_2H_5NHCH_3$. The effective Stark cell spacing, which allows calibration of the applied ac Stark electric field, was determined by utilizing the $J = 2 \leftarrow 1$ transition of OCS and Muenter's value[6] for its dipole moment of 0.715 21 D.

Due to C_s symmetry, normal $B_2H_5NHCH_3$ has dipole moment components only along the a and c axes. Each $2 \leftarrow 1$ transition gives rise to two Stark lobes, $M_J = 0$ and $M_J = 1$, for a total of six lobes for the three studied transitions. A least-squares fitting program was used to find the best values of μ_a^2 and μ_c^2 as solutions to the six simultaneous equations in the two unknowns. The Stark coefficients as well as least-squares-fitted slopes of $\Delta\nu$ vs E^2 curves for each of these six lobes are given in Table V. Derived values for the dipole moment components are $\mu_a = 2.50 \pm 0.02$ D, $\mu_c = 1.07 \pm 0.04$ D, and $\mu_{total} = 2.72 \pm 0.03$ D. The quoted errors represent the standard deviations for the solutions of the six simultaneous equations.

Molecular Structure

The Kraitchman substitution method used in this structural determination requires only the changes in moments of inertia upon isotopic substitution at an atom in order to calculate the coordinates of that particular atom, in the principal axis system of the reference species.[7] Principal axis coordinates were calculated for all atoms except the methyl group by using the Kraitchman method, with the 11–11–14 molecule as reference species. The results are tabulated in Table VI. The given uncertainties reflect errors in measured transition frequencies. These reported deviations become larger as an atom gets closer to a principal axis. For example, the a coordinates for the boron, H_N, and nitrogen atoms are −0.9171, and 0.2289, and 0.1464 Å while their uncertainties vary as ±0.0004, ±0.0012, and ±0.0034 Å, respectively. The coordinates of the H_{cis}, H_{trans}, and H_μ atoms have large uncertainties since c-type transitions, which are sensitive to A, were not observed. Again as seen in Table VI, the H_{trans} and H_μ atoms show reasonable deviations of ±0.0007 to ±0.0013 Å in their a coordinates, respectively, while larger deviations in their b and c coordinates reflect the larger uncertainties in their A constants. The large deviation of ±0.0053 Å in the a coordinate of the H_{cis} atom is attributed to the small value of that coordinate.

From the principal axis coordinates listed in Table VI, a geometry was calculated for (methylamino)diborane. Structural parameters for all three amino analogues are shown and compared

Table VI. Atomic Coordinates in the Principal Axis System of Normal $B_2H_5NHCH_3$

atom	a, Å	b, Å	c, Å
B_1	−0.9171 (04)	−0.9578 (04)	0.1320 (27)
B_2	−0.9171 (04)	0.9578 (04)	0.1320 (27)
N	0.1464 (34)	0.000[a]	−0.4315 (12)
H_μ	−1.7663 (13)	0.000[a]	0.6074 (37)
C	1.4805[b]	0.000[a]	0.1731[b]
H_6	1.3736[b]	0.000[a]	1.2579[b]
H_7	2.0270[b]	−0.8902[b]	−0.1385[b]
H_8	2.0270[b]	0.8902[b]	−0.1385[b]
H_N	0.2289 (12)	0.000[a]	−1.4382 (02)
$H_{cis,1}$	−0.5427 (53)	−1.5339 (17)	1.1324 (31)
$H_{trans,1}$	−1.5682 (07)	−1.5158 (07)	−0.6902 (18)
$H_{trans,2}$	−1.5682 (07)	1.5158 (07)	−0.6902 (18)
$H_{cis,2}$	−0.5427 (53)	1.5339 (17)	1.1324 (31)

[a] Assumed to be in the symmetry plane of the C_s point group. [b] Calculated by assuming a tetrahedral angle of 109.5° and r_{C-H} = 1.091 Å.

Table VII. Experimental and MNDO[a] Molecular Structure Parameters in $B_2H_5NHCH_3$ and Related Molecules

	$B_2H_5NH_2$[3]	$B_2H_5NHCH_3$ (this work)	$B_2H_5N(CH_3)_2$[4]
	Bond Lengths (Å)		
B–B	1.916 (2)	1.916 (1)	1.916 (4)
	(1.966)	(1.958)	(1.949)
B–N	1.558 (1)	1.538 (4)	1.544 (10)
	(1.558)	(1.571)	(1.585)
B–H_μ	1.355 (5)	1.365 (4)	1.365 (6)
	(1.374)	(1.371)	(1.369)
B–H_{cis}	1.193 (1)	1.214 (8)	1.191 (6)
	(1.171)	(1.171)	(1.172)
B–H_{trans}	1.193 (1)	1.188 (4)	1.191 (6)
	(1.171)	(1.172)	(1.172)
N–H_N	1.005 (6)	1.010 (2)	
	(1.009)	(1.016)	
N–C		1.51 (1)	1.49 (1)
		(1.488)	(1.501)
	Bond Angles (deg)		
B–H_μ–B	90.0 (06)	89.1 (02)	89.1 (09)
	(91.4)	(91.1)	(90.8)
B–N–B	75.9 (01)	77.0 (03)	76.8 (10)
	(78.2)	(77.1)	(75.9)
H_{cis}–B–H_{trans}	121.0 (03)	121.1 (03)	119.6 (05)
	(121.5)	(121.4)	(120.9)
H–N–H	111.0 (12)		
	(108.5)		
H_N–N–C		109.7 (13)	
		(108.3)	
C–N–C			110.0 (10)
			(111.1)
H_μ–N–H_N	124.5 (12)	122.6 (11)	
	(125.8)	(119.2)	
H_μ–N–C		127.7 (12)	125.0 (10)
		(132.5)	(124.5)
	Dipole Moment (D)		
μ_a	0.00	2.50 (02)	2.77 (02)
	(0.03)	(2.79)	(3.22)
μ_b	2.67 (03)	0.00	0.00
	(2.94)	(0.00)	(0.00)
μ_c	0.00	1.07 (04)	0.00
	(0.00)	(1.48)	(0.00)
μ_{total}	2.67 (03)	2.72 (03)	2.77 (02)
	(2.94)	(3.15)	(3.22)

[a] MNDO-calculated values are in parentheses below the experimental values.

(6) Muenter, J. S. *J. Chem. Phys.* **1968**, *48*, 4544.
(7) Kraitchman, J. *Am. J. Phys.* **1951**, *21*, 17.

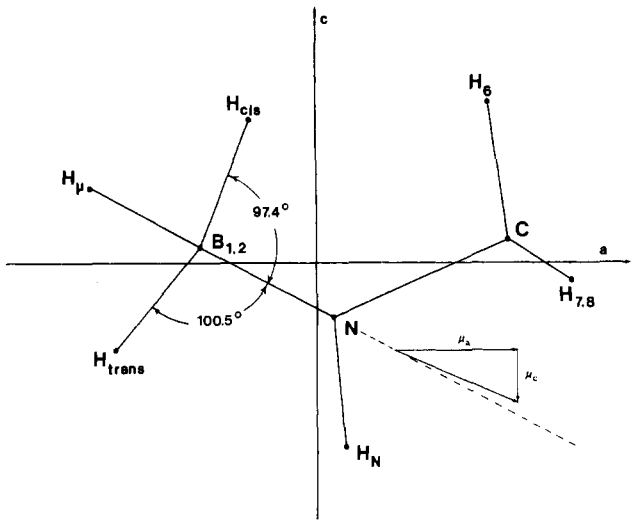

Figure 2. Projection in the *ac* plane in the normal species of (methylamino)diborane.

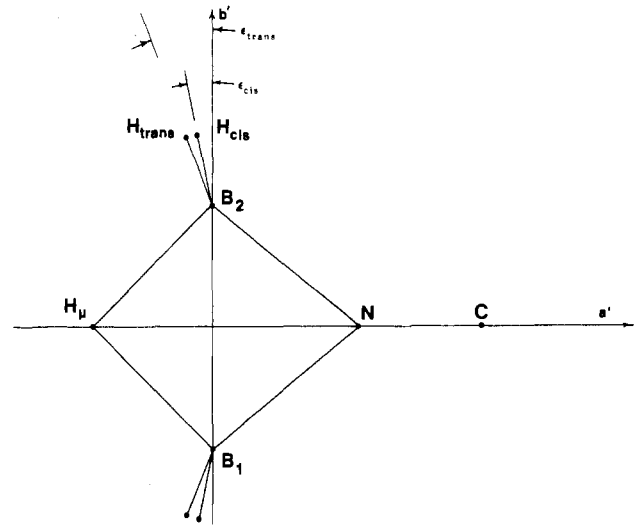

Figure 3. Projection in the B_1–N–B_2–H_μ plane in the normal species of (methylamino)diborane. The *a'* axis represents the rotation of the principal *a* axis in the *ac* plane (see Figure 2) such that the H_μ–N vector contains the *a'* axis. The *b'* axis is an axis parallel to the principal *b* axis.

in Table VII. From the Cartesian coordinates included in this paper, any other structural parameters desired can be easily calculated. The B–B bond lengths are identical in all three cases within the experimental uncertainties. The B–N bond lengths appear to decrease slightly as methyl groups are added across the series, although the larger uncertainty in the $B_2H_5N(CH_3)_2$ work makes such a statement tenuous. Little differences are noted for B–H_μ or N–H_N bond lengths proceeding through the series. With use of both center-of-mass conditions and fitting to the derived moments of inertia, the methyl group was located and coordinates were calculated for the carbon atom. Results agreed closely between these two methods, giving values of 1.508 ± 0.005 Å for the C–N bond length and 128.3 ± 1.2° for the H_μ–N–C bond angle by fitting to the center-of-mass conditions, while values of 1.510 ± 0.002 Å and 127.1 ± 1.1° resulted for the same parameters by fitting to the moments of inertia. This approximate calculated value of 1.51 ± 0.01 Å for the C–N bond length agrees well with the earlier reported value of 1.49 ± 0.01 Å in $B_2H_5N(CH_3)_2$. Both the B_1–H_μ–B_2 and B_1–N–B_2 bond angles appear very similar throughout the series. The same holds for the angle H–B–H, which varies from 119.6 ± 0.5 to 121.1 ± 0.3°. The dipole moments reported in Table VII show that the value of 2.72 ± 0.03 D found in $B_2H_5NHCH_3$ is the average of 2.67 ± 0.03 and 2.77 ± 0.02 D reported for the other two amino compounds. Since the nitrogen atom is more electronegative than the boron atoms, a small negative charge is located here. The methyl group is expected to contribute little to the charge separation in this molecule. The direction of the dipole moment is thus selected as shown in the inset in Figure 2. The total dipole moment lies mostly in the B_1–H_μ–B_2–N plane, with a small component in the direction of the methyl group.

Projections of $B_2H_5NHCH_3$ in selected planes permit clearer visualization of some of these structural parameters. Figure 2 shows the *ac* plane, in which the five atoms H_μ, N, H_N, C, and H_6 lie. The bond angle H_{trans}–B–N projected in the *ac* or symmetry plane is 100.5 ± 0.5°, while the projected angle H_{cis}–B–N is 97.4 ± 0.6°. In response to the initially posed question of planarity, it is interesting to note that, in spite of this difference in bond angles, the H_μ atom appear to be unaffected and the B_1–H_μ–B_2 and the B_1–N–B_2 planes are coplanar within the experimental uncertainty (±1.0°). Earlier work[3,4] on $B_2H_5NH_2$ and $B_2H_5N(CH_3)_2$ discussed the angle ϵ, defined as the angle made by the BH_2 plane and the plane perpendicular to the C_{2v} symmetry axis in those molecules. There are two analogous values of this angle in $B_2H_5NHCH_3$, owing to symmetry reduction to the C_s point group. The angle formed between the B_1–B_2 vector and projections of the B–H_{cis} vector in the B_1–H_μ–B_2–N central plane is called ϵ_{cis}, while the analogous angle for H_{trans} is called ϵ_{trans}, both are shown in Figure 3. The H_{cis} atom and the H_{trans} atom belonging to a particular boron atom are not superimposed in such a projection, while they would indeed be superimposed in similar projections in the other two molecules, $B_2H_5NH_2$ and $B_2H_5N(CH_3)_2$. Values calculated are ϵ_{cis} = 13.5 ± 0.2° and ϵ_{trans} = 18.8 ± 0.5°. These results may be compared to the ϵ values of 16.8 ± 0.1 and 16.7 ± 1.0° reported in the $B_2H_5NH_2$ and $B_2H_5N(CH_3)_2$ work, respectively.

Table VIII. Kraitchman Substitution Schemes for Independent Determinations of B, N, and H_N Geometries in (Methylamino)diborane Using Two Different Reference Molecules

ref molecule	*r*(B–B), Å	*r*(B–N), Å	*r*(N–H_N), Å
11–11–14	1.9157 (07)	1.5382 (44)	1.0101 (21)
11–10–14	1.9157 (07)	1.5474 (98)	1.0105 (43)

Table IX. Kraitchman Substitution Schemes for Three Independent B–B Bond Length Determinations in (Methylamino)diborane

ref molecule	substituted molecule	*r*(B–B), Å
11–11–14	11–10–14	1.9157 (07)
11–11–15	11–10–15	1.9156 (10)
11–11–14–D_N	11–10–14–D_N	1.9164 (12)

To determine the accuracy of structural parameters from these microwave measurements, both the 11–11–14 and 11–10–14 species were used as reference molecules for Kraitchman calculations. With use of the reference species shown in Table VIII, coordinates were calculated for the atoms B_1, B_2, N, and H_N. The bond lengths B–B, B–N, and N–H_N thus each had two independent determinations. Since the 11–10–14 molecule does not have C_s symmetry, both the nitrogen and H_N atoms are not contained in the *ac* plane, and both should have small, non-zero *b* coordinates. However, the Kraitchman method is insensitive to such small distances from the principal axes and the actual calculations showed characteristic imaginary values for these *b* coordinates. Values of zero were, therefore, used with resulting large uncertainties in the calculated bond lengths, especially in *r*(B–N). Values for the other two parameters (B–B, N–H_N) agree very well for these two schemes. Similarly, the B–B bond length had three independent determinations when the pairs (11–11–14, 11–10–14), (11–11–15, 11–10–15), and (11–11–14–D_N, 11–10–14–D_N) were entered into Kraitchman programs. Since all three reference species now have C_s symmetry, unlike 11–10–14, no problems are encountered with atoms lying too close to a principal axis. Also, only the *b* coordinate enters into the B–B bond length calculations as seen from Figure 1. Small deviations of only ±0.001 Å resulted, and this set of values is reported in Table IX. These differences reflect zero-point energy differences due to isotopic substitution, which are the limiting factors in all microwave structural determinations.[8]

Discussion

The first consequence of having two different terminal groups (–H, $-CH_3$) on the nitrogen atom in $B_2H_5NHCH_3$ is to lower the symmetry from the C_{2v} found in both $B_2H_5NH_2$ and $B_2H_5N(CH_3)_2$ to that of the C_s point group. One important result from such symmetry lowering is to permit the appearance of a second dipole moment component. For a molecule with C_{2v} symmetry, the permanent dipole moment must be directed entirely along the C_{2v} axis. However, for the case of C_s symmetry, the total dipole moment is now contained in the symmetry plane with possible components along two of the three principal axes necessarily contained within such a plane. The case for $B_2H_5NHCH_3$ is such that $\mu_a = 2.50 \pm 0.02$ D and $\mu_c = 1.07 \pm 0.04$ D, which has permitted observation of not only *a*-type but also *c*-type transitions. Thus, better values for the rotational constants (*A*, *B*, *C*) can be calculated for isotopic species of $B_2H_5NHCH_3$ than would be possible in the absence of observed *c*-type transitions, considering the observed range of asymmetry parameters seen in Table IV. As the symmetry of the molecule increases, the *a*-type transitions become less and less dependent on the *A* constant and any least-squares fitting process would show larger standard deviations in the *A* constant. Such deviations were not encountered in the earlier $B_2H_5NH_2$ work since asymmetry parameters were smaller, varying between –0.24 and +0.08. Similarly, for the previous $B_2H_5N(CH_3)_2$ work, an even narrower range of asymmetry parameters was found, all values centering about zero.

MNDO calculations were performed by employing a previously described standard procedure[9] modified for a CDC 170 computer. The input geometries of the three derivatives in the aminodiborane series, $B_2H_5NH_2$, $B_2H_5NHCH_3$, and $B_2H_5N(CH_3)_2$, were based upon the structures determined by microwave spectroscopy. In all input geometries the B_1–N–B_2–H_μ ring was held planar and the bisecting planes formed by the ring and the amino group (N and its two coordinating atoms) were constrained to be perpendicular. All other parameters were optimized.

In Table VII, the MNDO-calculated geometries of all three derivatives are compared to those obtained by microwave spectroscopy.[3,4] The calculated bond lengths and bond angles of all derivatives were consistent with those of the experimental data, with standard deviations of 0.015 Å and 1.27°, respectively. MNDO calculated the B–N and B–H_μ bond lengths reasonably well, considering that MNDO has a tendency to underestimate the strength of three-center bonds.[10]

Also, in Table VII, the MNDO-calculated and experimentally obtained dipole moments are compared. As can be seen, the order of magnitude of the calculated dipole moment components and total dipole moment is reasonably good, with a maximum deviation from experimental results of 0.5 D. The relative trend in the magnitude of the total dipole moments is as experimentally observed.

These calculated results demonstrate the utility of MNDO in the prediction of structures and dipole moments to assist in the determination of the general nature of the expected spectra of boron hydride derivatives for microwave spectroscopy. The first amino analogue studied, $B_2H_5N(CH_3)_2$, had the nitrogen atom located too close to the center of mass of the molecule for an accurate substitution structure to be calculated for any structural parameter involving the nitrogen atom position. Later work on $B_2H_5NH_2$, a more difficult molecule to deal with from both a thermal stability and hydrolysis point of view, resolved this question, produced a fairly accurate nitrogen atom coordinate, and permitted confirmation of planarity and C_{2v} character. An interesting question that arose was whether or not planarity would remain in force if a single methyl substitution were made at the nitrogen atom. Results from this study show that indeed planarity remains in effect as the B_1–H_μ–B_2 and the B_1–N–B_2 planes are coplanar within about 1.0°. This is within the experimental uncertainty and reflects the previously mentioned accumulated errors.

Acknowledgment. We gratefully acknowledge support of the Army Research Office under Grant No. DAAL03-86-K0172. We gratefully acknowledge the NSF for the instrumentation grant for the VAX 780 computer, on which these calculations were carried out, and also the USC Loker Hydrocarbon Institute for partial funding of this project. E.V.O. also wishes to gratefully acknowledge the California State University Computer Science Facility for unfunded time on the CDC Cyber 760 computer and to thank Dr. J. J. P. Stewart for numerous invaluable discussions on the use of the MNDO program. We also thank David Harris for the long-term loan of a Hewlett-Packard microwave spectrometer, upon which portions of this work were carried out.

Registry No. $B_2H_5NHCH_3$, 27073-27-4; $B_2H_5NHCH_3$ (^{11}B,^{11}B,^{14}N), 111348-88-0; $B_2H_5NHCH_3$ (^{11}B,^{10}B,^{14}N), 111323-89-8; $B_2H_5NHCH_3$ (^{11}B,^{11}B,^{15}N), 111323-90-1; $B_2H_5NHCH_3$ (^{11}B,^{10}B,^{15}N), 111323-91-2; $B_2H_5NHCH_3$ (^{11}B,^{11}B,^{14}N,D_N), 111323-92-3; $B_2H_5NHCH_3$ (^{11}B,^{10}B,^{14}N,D_N), 111323-93-4; $B_2H_5NHCH_3$ (^{11}B,^{11}B,^{14}N,D_{cis}), 111323-94-5; $B_2H_5NHCH_3$ (^{11}B,^{11}B,^{14}N,D_{trans}), 111408-43-6; $B_2H_5NHCH_3$ (^{11}B,^{11}B,^{14}N,D_μ), 111323-95-6.

(8) Townes, C. H.; Schawlow, A. L. *Microwave Spectroscopy*; McGraw-Hill: New York, 1955.
(9) Dewar, M. J. S.; Thiel, W. *J. Am. Chem. Soc.* **1977**, *99*, 4899.
(10) Dewar, M. J. S.; McKee, M. L. *Inorg. Chem.* **1978**, *17*, 1569.